Experimental and Molecular Pathology 135 (2024) 104882

Contents lists available at ScienceDirect

Experimental and Molecular Pathology

journal homepage: www.elsevier.com/locate/yexmp

An *in-silico* analysis reveals further evidence of an aggressive subset of lung carcinoids sharing molecular features of high-grade neuroendocrine neoplasms

Giuseppe Pelosi [a,b,*,1], Valentina Melocchi [c], Elisa Dama [c], Paul Hofman [d], Marco De Luca [b], Adriana Albini [e], Maria Gemelli [f], Riccardo Ricotta [f], Mauro Papotti [g], Stefano La Rosa [h], Silvia Uccella [i], Sergio Harari [j,k], Angelica Sonzogni [l], Michael K. Asiedu [m], Dennis A. Wigle [m], Fabrizio Bianchi [c,**,1]

[a] *Department of Oncology and Hemato-Oncology, University of Milan, Milan, Italy*
[b] *Inter-Hospital Pathology Division, Istituto di Ricovero e Cura a Carattere Scientifico (IRCCS) MultiMedica, Milan, Italy*
[c] *Unit of Cancer Biomarkers, Fondazione IRCCS Casa Sollievo della Sofferenza, San Giovanni Rotondo, FG, Italy*
[d] *Laboratory of Clinical and Experimental Pathology, Biobank BB-0033-00025 and Centre Hospitalier Universitaire de Nice, FHU OncoAge, Université Côte d'Azur, 06100 Nice, France*
[e] *IEO European Institute of Oncology IRCCS, Milan, Italy*
[f] *Medical Oncology Unit, Istituto di Ricovero e Cura a Carattere Scientifico (IRCCS) MultiMedica, Milan, Italy*
[g] *Department of Oncology, University of Turin, Turin, Italy*
[h] *Pathology Unit, Department of Medicine and Surgery, University of Insubria, Varese, Italy*
[i] *Department of Biomedical Sciences, Humanitas University, Rozzano, Milan, Italy*
[j] *Department of Medical Sciences and Community Health, University of Milan, Milan, Italy*
[k] *Division of Pneumology, Istituto di Ricovero e Cura a Carattere Scientifico (IRCCS) MultiMedica, Milan, Italy*
[l] *Department of Pathology and Laboratory Medicine, IRCCS Istituto Nazionale dei Tumori, Milan, Italy*
[m] *Division of General Thoracic Surgery, Department of Surgery, Mayo Clinic College of Medicine, Rochester, MN, USA*

ARTICLE INFO

Keywords:
SCLC
LCNEC
Carcinoid
Signature
Survival
Progression

ABSTRACT

Little is known as to whether there may be any pathogenetic link between pulmonary carcinoids and neuroendocrine carcinomas (NECs). A gene signature we previously found to cluster pulmonary carcinoids, large cell neuroendocrine carcinoma (LCNEC) and small cell lung carcinoma (SCLC), and which encompassed *MEN1, MYC, MYCL1, RICTOR, RB1, SDHA, SRC* and *TP53 mutations or* copy number variations (CNVs), was used to reclassify an independent cohort of 54 neuroendocrine neoplasms (NENs) [31 typical carcinoids (TC), 11 atypical carcinoids (AC) and 12 SCLC], by means of transcriptome and mutation data. Unsupervised clustering analysis identified two histology-independent clusters, namely CL1 and CL2, where 17/42 (40.5%) carcinoids and all the SCLC samples fell into the latter. CL2 carcinoids affected survival adversely, were enriched in T to G transversions or T > C/C > T transitions in the context of specific mutational signatures, presented with at least 1.5-fold change (FC) increase of gene mutations including *TSC2*, *SMARCA2*, *SMARCA4*, *ERBB4* and *PTPRZ1*, differed for gene expression and showed epigenetic changes in charge of *MYC* and *MTORC1* pathways, cellular senescence, inflammation, high-plasticity cell state and immune system exhaustion. Similar results were also found in two other independent validation sets comprising 101 lung NENs (24 carcinoids, 21 SCLC and 56 LCNEC) and 30 carcinoids, respectively. We herein confirmed an unexpected sharing of molecular traits along the spectrum of lung NENs, with a subset of genomically distinct aggressive carcinoids sharing molecular features of high-grade neuroendocrine neoplasms.

* Correspondence to: G. Pelosi, Inter-Hospital Pathology Division, Science & Technology Park, IRCCS MultiMedica, Via Gaudenzio Fantoli 16/15, 20138 Milan, Italy.
** Correspondence to: F. Bianchi, Unit of Cancer Biomarkers, Fondazione IRCCS Casa Sollievo della Sofferenza, Viale Padre Pio 7, 71013 San Giovanni Rotondo, Italy.
E-mail addresses: giuseppe.pelosi@unimi.it (G. Pelosi), f.bianchi@operapadrepio.it (F. Bianchi).
[1] Co-corresponding authors.

https://doi.org/10.1016/j.yexmp.2024.104882
Received 8 August 2023; Received in revised form 23 December 2023; Accepted 15 January 2024
Available online 20 January 2024

1. Introduction

Carcinoids of the lung are well-differentiated neuroendocrine tumors (NETs), which are split into typical carcinoid (TC)/NET G1 and atypical carcinoid (AC)/NET G2 by means of mitotic count per 2 mm^2 and punctate necrosis assessment on surgical resection specimens (Travis et al., 2021). In turn, neuroendocrine carcinomas (NECs) are high-grade (poorly differentiated) neoplasms, featuring either small (small cell lung carcinoma (SCLC)) or large cells (large cell neuroendocrine carcinoma (LCNEC)) (Beasley et al., 2021; Rekhtman, 2022; Rekhtman et al., 2021). SCLC is most often diagnosed in biopsy or cytology samples (Beasley et al., 2021; Luchtenborg et al., 2014; Petrella et al., 2022; Rekhtman, 2022; Rekhtman et al., 2021), while LCNEC is seen in surgical and non-surgical metastatic setting, with survival and prognosis that is more akin to SCLC that conventional non-small cell carcinoma (NSCC) (Rekhtman et al., 2021). Whether resectable and unresectable NECs (Luchtenborg et al., 2014) mirror the same or different diseases is still matter of speculation (Metovic et al., 2021a; Metovic et al., 2021b; Pelosi et al., 2019). Currently, NETs and NECs are considered distinct and separate tumor entities across the spectrum of lung neuroendocrine neoplasms (NENs) with neither molecular overlap nor common developmental continuum (Beasley et al., 2021; Papotti et al., 2021; Rekhtman et al., 2021; Travis et al., 2021). Quite unexpectedly (Alcala et al., 2019; Cros et al., 2021; Dinter et al., 2019; Fabbri et al., 2017; Pelosi et al., 2021; Pelosi et al., 2018; Pelosi et al., 2019; Peng et al., 2022; Simbolo et al., 2019; Vollbrecht et al., 2015), however, NETs and NECs have been reported in the lung (Alcala et al., 2019; Cros et al., 2021; Pelosi et al., 2018; Pelosi et al., 2019; Peng et al., 2022; Simbolo et al., 2019; Vollbrecht et al., 2015), thymus (Dinter et al., 2019; Fabbri et al., 2017) and gastroenteropancreatic tract (Pelosi et al., 2021) to share most of the same altered genes, yet with different prevalence rates. These findings could support the view that at least a subset of NECs featuring either SCLC or LCNEC might actually progress from pre-existing NETs.

In this regard, we previously observed that a gene signature, including *KRAS, MEN1, MYC, MYCL1, RICTOR, RB1, SDHA, TERT* and *TP53* mutations and copy number variations (CNVs), was effective to group NETs and NECs in the same unsupervised clusters (Pelosi et al., 2018). This molecular tight association would support the speculation that the fate of some stochastically transformed NETs could be to generate NECs (Pelosi et al., 2018) or at least it would suggest a common natural history driven by interaction of individual risk factors and patient variables leading to aggressive NENs (Pelosi, 2022).

In this study, we further confirm that a subset of carcinoids closely clustered due to shared transcriptomic and mutation features with NECs as heralded by stochastic acquirement of epigenetic and genetic alterations. These findings, even if not formally demonstrated with functional genomic experiments, could support the interesting working hypothesis of secondary high-grade (poorly differentiated) NENs, i.e., secondary NECs, as an unexpected paradigm shift to the perceived lack of pathogenetic link between pulmonary carcinoids and NECs (Metovic et al., 2021a; Metovic et al., 2021b; Pelosi et al., 2019; Pelosi et al., 2017).

2. Material and methods

2.1. Tumor patients

This study comprised a primary cohort of 54 lung NENs belonging to 31 TC, 11 AC and 12 SCLC fulfilling criteria of the World Health Organization (WHO) classification (Travis et al., 2021), all surgically resected specimens with no neoadjuvant treatment administration, which had previously been published by Asiedu et al. (Gene Expression Omnibus – GEO – database accession #: GSE108055) (Asiedu et al., 2018). A second cohort of 101 lung NENs (24 carcinoids, 21 SCLC and 56 LCNEC) obtained from GEO database (accession #: GSE30219) (Rousseaux et al., 2013) and a third independent cohort of 30 lung carcinoids downloaded from GEO database (accession#: GSE118131) (Laddha et al., 2019) were included in the study for validation testing.

2.2. Study design

This is an in-silico study aimed to investigate an innovative concept of secondary pulmonary NET transformation into SCLC, with insights into the genetic and epigenetic changes involved in the transition. Previously, we found out by unsupervised clustering that a gene signature comprising *KRAS, MEN1, MYC, MYCL1, RICTOR, RB1, SDHA, TERT* and *TP53* mutations and CNVs, in turn derived from a list of 27 recurrently mutated genes and 13 CNVs, was able to tightly cluster carcinoids and NECs, thus suggesting a pathogenetic link between these tumors (Pelosi et al., 2018). Transcriptomic data, however, were lacking in that investigation (Pelosi et al., 2018), which could have provided useful information about transcriptional signatures hallmarking relevant cancer pathways involved in such an evolution. In this study, we have further explored such gene signature (Pelosi et al., 2018) in another independent data set comprising carcinoids and SCLC (Asiedu et al., 2018) to test its ability to discriminate subsets of carcinoids closely clustering resectable SCLC. Since *TERT* was not included in the cases studied by Asiedu, it was replaced by *SRC* gene expression data, which is known to play a pivotal role in cancer development and progression (Parker et al., 1981) and belonged to our previously observed 13 CNVs in lung carcinoids (Pelosi et al., 2018). Results were validated in two other independent data sets obtained from GEO database [accession #: GSE30219 (Rousseaux et al., 2013) and accession#: GSE118131 (Laddha et al., 2019)] totaling 101 lung NENs and 30 pulmonary carcinoids, respectively.

2.3. Bioinformatics and statistics

Normalized gene expression data were downloaded from Gene Expression Omnibus (GEO) database (GSE108055) and were applied to: i) hierarchical clustering analysis (Pelosi et al., 2021; Pelosi et al., 2018); ii) Gene-Set Enrichment Analysis (GSEA, https://www.gsea-msigdb.org/gsea/index.jsp); and iii) CIBERSORTx (Newman et al., 2019) analysis. Whole exome sequencing fastq files of 12 carcinoid samples and corresponding normal samples from Asiedu et al. (Asiedu et al., 2018) were aligned using BWA (Li and Durbin, 2009) and hg19 as reference genome. Somatic mutations were retrieved using Mutect2 (Van der Auwera et al., 2013) and then were filtered to retain the most informative ones (see Supplementary Information for further details). Filtered somatic mutations were used to perform Single Base Substitution (SBS) Signatures analysis (Alexandrov et al., 2020). Hierarchical clustering analysis (Pelosi et al., 2021; Pelosi et al., 2018) and Gene-Set Enrichment Analysis (GSEA, https://www.gsea-msigdb.org/gsea/index.jsp) were applied also to normalized gene expression data of GSE30219. JMP 16 (JMP®, Version 16. SAS Institute Inc., Cary, NC, 1989–2019) and SAS software, version 9.4 (SAS Institute, Inc., Cary, NC) were used for all statistical analyses and relative plots. All *p*-values were two-sided and p-values <0.05 were considered as significant.

Further details can be found in Supplementary Material.

3. Results

3.1. Hierarchical clustering revealed two distinct groups of carcinoids

Since gene expression profile is highly associated to CNVs (Shao et al., 2019), we focused on the same gene set we previously showed to comprise CNVs in lung carcinoid tumors, which had contributed to outline NEN subsets (Pelosi et al., 2018). In particular, we started analyzing the expression profile of this signature comprising *MEN1, MYC, MYCL1, RICTOR, RB1, SDHA, TP53, TERT* and *SRC genes* by using microarray gene expression data on an independent 54 lung NEN cohort

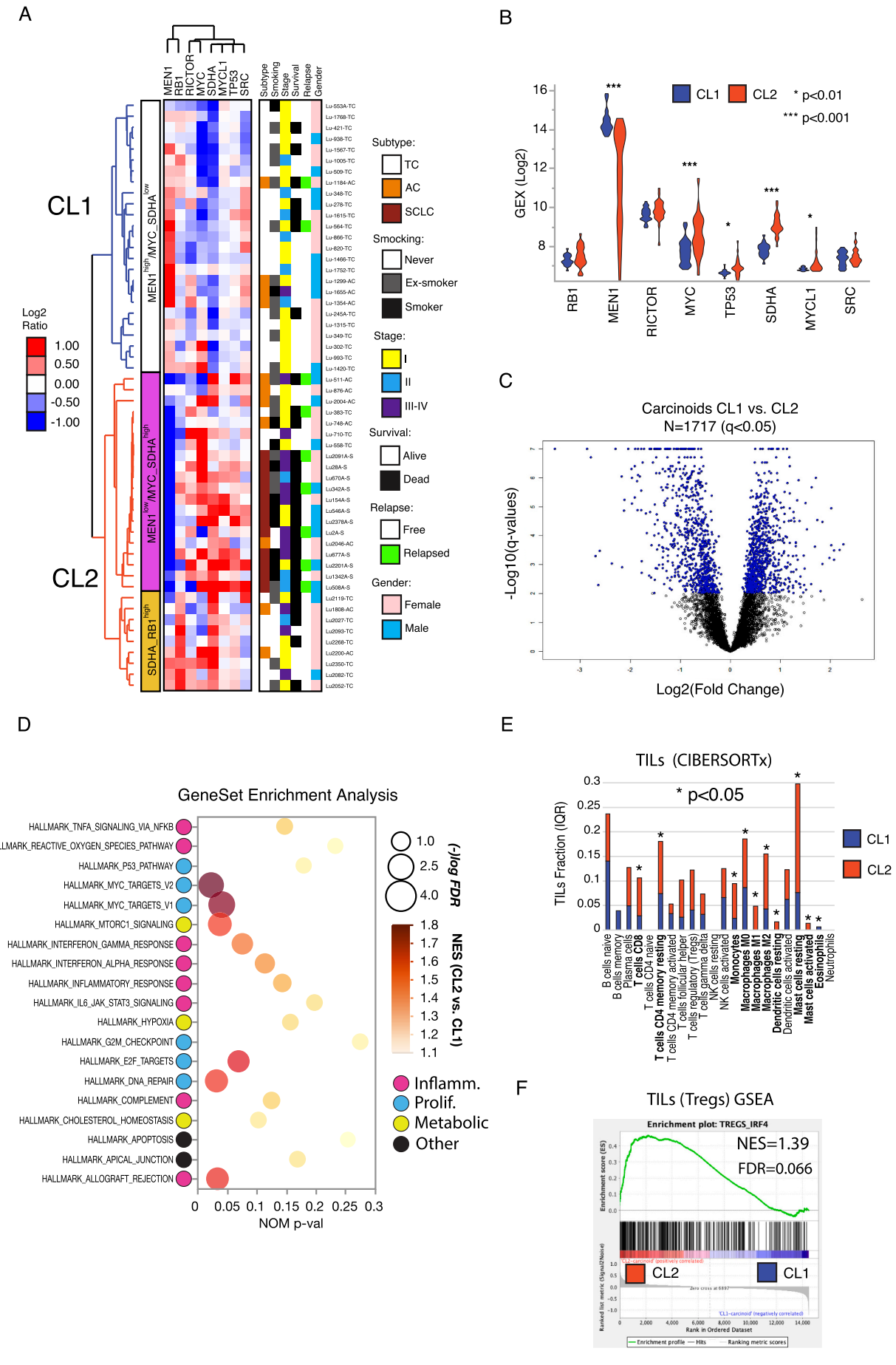

(caption on next page)

Fig. 1. A. Hierarchical clustering analysis of the expression of the gene signature in the cohort of 54 NENs. The first branch of the dendrogram was color-based and represents the two main clusters (CL1 and CL2) identified. The prevalent gene expression pattern of the gene signature is indicated underneath the dendrogram. Color codes of the heatmap and of the main clinical-pathological information are as per the legend. B. Violin plots of the gene signature expression regulation in CL1 vs. CL2 clusters of lung NENs. Asterisks indicate statistically significant differences. *P*-values were calculated by Wilcoxon test. C. Volcano plot of differentially expressed genes among CL1- vs. CL2-carcinoids. Blue dots represent statistically significant genes ($N = 1717$; q-value<0.05). D. Bubble plot of the Hallmark GeneSets found enriched in CL2-carcinoids by Gene Set Enrichment Analysis (GSEA). Colors of the bubbles represent the magnitude of enrichment (NES, normalized enrichment score) and are as per the legend. Size of the bubbles represents the statistical significance of the enrichment (FDR, false-discovery-rate based on 1000 random permutation), i.e., the bigger the most significant and are as per the legend. Y-axes, Gene Sets. GeneSets were also labelled according to their overall biological function i.e., Inflammatory (Pink), Proliferative (Light blue), Metabolic (Yellow) or other (Black). X-axes, nominal *p*-values. E. CIBERSORTx analysis of TIL expression signatures. Y-axes, inter-quartile range (IQR) of the estimated fraction of TILs in CL1- or CL2-carcinoids. X-axes, subsets of TILs. Color code is as per the legend. Asterisks indicate statistical significance ($p < 0.05$; Wilcoxon test). F. GSEA of Tregs IRF4+ specific signature in CL2-carcinoids vs. CL1-carcinoids. NES, normalized enrichment score. FDR, false-discovery rate. (For interpretation of the references to color in this figure legend, the reader is referred to the web version of this article.)

(see Materials and Methods). However, as TERT expression was not reported in this dataset, it was excluded from the analysis. Supervised clustering analysis according to the current histologic classification (Beasley et al., 2021; Papotti et al., 2021; Rekhtman et al., 2021; Travis et al., 2021) revealed a sharp enucleation of SCLC in the expression levels of *MEN1*, *MYC*, *TP53*, *SDHA* and *MYCL1* among subtypes, whereas no differences emerged among carcinoids (Fig. S1 A,B). However, when we performed unsupervised clustering analysis by the same gene set, we identified two distinct clusters of neoplasms, namely CL1 and CL2, which totaled the entire 54-tumor cohort (Fig. 1 A). The clusters CL1 and CL2 comprised 25 and 29 patients, respectively, and showed distinct expression patterns according to the relevant gene signature. The cluster CL1 was dominated by $MEN1^{high}$/MYC_$SDHA^{low}$ expression, whereas the cluster CL2 featured two closely related subsets of NENs showing SDHA_$RB1^{high}$ and $MEN1^{low}$/MYC_$SDHA^{high}$ expression patterns, respectively (Fig. 1 A-B). Of note, CL2 grouped all the 12 SCLC cases under the $MEN1^{low}$/MYC_$SDHA^{high}$ pattern ($p < 0.0001$), whereas there was just a trend ($p = 0.09$) for TC to populate CL1 (84% TC,16% AC) and for AC to localize in CL2 (59% TC, 41% AC, after exclusion of SCLC cases) (Table 1).

Subsequently, we investigated the whole-transcriptome of CL1 and CL2 carcinoids. Overall, we found a total of 1717 differentially regulated genes (q-value<0.05, multivariate 1000 random permutation test) (Fig. 1C; Fig. S1C), including several neuroendocrine markers such as chromogranins and synaptophysin which were significantly down-regulated in CL2 carcinoids (Supplementary Table 1A). Of note, when we intersected this 1717-gene set with another gene set, which was differentially regulated in SCLC vs. CL1 carcinoids ($N = 4590$), a total of 1518 genes were found in common (88%, *p*-value ≤0.0001; Exact hypergeometric probability with normal approximation), thereby further supporting shared expression traits of CL2 carcinoids with SCLC (Supplementary Table 1B). When we investigated by Gene Set Enrichment Analysis (GSEA; see Materials and Methods) a collection of transcriptional signatures, which are hallmarks of well-defined biological states or processes (i.e., 'Hallmark GeneSets'), we found that several proliferation-related gene sets, such as Myc, E2f, DNA repair, p53 pathway and G2M-checkpoint, turned out enriched in CL2 carcinoids (Fig. 1 D). Intriguingly, gene sets involved in inflammation were enriched in CL2 carcinoids as well (Fig. 1 D), thus suggesting an altered immune landscape (e.g., tumor infiltrating lymphocytes or TILs) in these CL2 carcinoids. Indeed, CIBERSORTx analysis revealed TIL-related expression signatures indicative of immune system exhaustion in CL2 carcinoids as heralded by increased CD8+ T cells, precursor monocytes, proinflammatory M1 macrophages, M2-polarized tumor-associated macrophages, CD4+ T cells, mast cells and dendritic cell resting (Fig. 1 E). Furthermore, a gene expression signature specific of intratumor CD4+ effector regulatory T cells (IRF4+ Tregs), which are known to suppress antitumor immune response and correlate with exhausted CD8+ T cell accumulation (Alvisi et al., 2020), was significantly enriched in CL2 carcinoids by GSEA (NES = 1.39; FDR < 0.1) (Fig. 1 F). Notably, when we performed GSEA comparing NECs (i.e., SCLC) with NETs (i.e., carcinoids), we found most of the enriched pathways overlapping with those enriched in NET-CL2 (Fig. S1D), further supporting the issue of similar molecular profile between C2-NETs and NECs.

Subsequently, we analyzed two additional independent cohorts of samples, the first encompassing 101 NENs (i.e., the GSE30219 cohort; see methods) among which 24 carcinoids, the second formed only by 30 carcinoids (i.e., the GSE118131 cohort; see methods). While applying our gene signature, we identified upon unsupervised clustering two distinct groups of NENs with pathologic and molecular features resembling the initial 54 lung NEN cohort (Fig. S2A,D). Notably, 4044 genes (18.6% out of total) were found to be significantly (q-value<0.05, multivariate 1000 random permutation test) and differentially expressed between CL1 ($N = 15$) and CL2 (N = 15) NENs subsets in the GSE118131 cohort (Fig. S3A). In particular, gene expression signatures of proliferation/pro-inflammation and high-plasticity cell state (HPCS) [e.g., epithelial mesenchymal transition (EMT), Notch signaling] were significantly enriched (FDR = 0.1; Fig. S3B, Fig. S3C) in these additional CL2 looking-carcinoids, thus further supporting the acquirement of aggressive molecular traits in these NETs.

3.2. Genetic alterations of NETs and impact on cell plasticity

Next, we analyzed the mutational profile of CL1 and CL2 carcinoids. Whole-exome sequencing data were available for a total of 12 carcinoids (see Material and Methods), of which eight clustered in CL2 and four in CL1. We examined the mutation frequency of genes we previously found to be mutated in lung NENs (27-gene signature) (Pelosi et al., 2018) in both CL1 and CL2 and observed a prevalence of *TP53*, *MEN1*, *NCAM2* and *KRAS* in the former and of *TSC2*, *SMARCA2*, *ERBB4*, *PTPRZ1* and *SMARCA4* mutations in the latter, respectively [in either cluster > |1.5| fold change (FC)] (Fig. 2 A). Notably, *SMARCA2* and *SMARCA4* are the catalytic members of the chromatin remodeler SWI/SNF complex, which is frequently altered in human malignancies (Kadoch et al., 2013) and whose alterations are able to modify the epigenetic landscape of tumor cells by favoring the acquirement of cell plasticity and the loss of cell identity in lung cancer (Chang et al., 2018; Concepcion et al., 2022; Rubin et al., 2020). In keeping with these findings, we observed downregulation of neuroendocrine (NE) markers and upregulation of AT2 club cell markers in CL2-carcinoids (Fig. 2 B, Supplementary Table 1B), which resembles the NE fate reprogramming of SCLC molecular subtypes characterized by enhanced aggressiveness potential and chemoresistance but more permissiveness to immunotherapy (Gay et al., 2021; Ireland et al., 2020; Rubin et al., 2020). In this regard, we observed enrichment in stem-cell related genes (Fig. S1 E) and a signature of HPCS (Fig. S1 F), which were shown to emerge during lung cancer progression (Marjanovic et al., 2020).

Lastly, we found an enrichment of T > G transversions (Fig. 2 C, Fig. S3 D), which is associated with tobacco smoke (Pleasance et al., 2010). More in depth, mutational signatures (Alexandrov et al., 2016) revealed a more homogeneously altered pattern in CL2 than CL1, with prevalence of SBS96B and SBS96E corresponding to clock-like patterning (mismatch repair) and haloalkane exposure, respectively, both of which were characterized by T > C or C > T transitions (Fig. 2 D).

Table 1
Association analysis of clusters and clinico-pathologic characteristics.

	All $N = 54$	Cluster			p-value	
		CL1 $N = 25$	CL2 $N = 29$	CL2 w/o SCLC $N = 17$	CL1 vs CL2	CL1 vs CL2 w/o SCLC
Age at surgery [yrs.]						
median (Q1;Q3)	61 (56;69)	61 (55;68)	61 (57;71)	61 (56;69)	0.31 [a]	0.75 [a]
min-max	31–86	31–77	41–86	41–84		
Gender						
male	20 (37.0%)	9 (36.0%)	11 (37.9%)	5 (29.4%)	1.00 [b]	0.75 [b]
female	34 (63.0%)	16 (64.0%)	18 (62.1%)	12 (70.6%)		
Smoking status						
never smoker	23 (42.6%)	13 (52.0%)	10 (34.5%)	9 (52.9%)		
former smoker	20 (37.0%)	10 (40.0%)	10 (34.5%)	6 (35.3%)	0.10 [b]	1.00 [b]
current smoker	11 (20.4%)	2 (8.0%)	9 (31.0%)	2 (11.8%)		
Pack-years						
median (Q1;Q3)	35 (20;70)	25 (12;62.5)	40 (25;70)	32.5 (20;57)	0.21 [a]	0.70 [a]
min-max	5–100	5–99	5–100	5–99		
Hystological type						
TC	31 (57.4%)	21 (84.0%)	10 (34.5%)	10 (58.8%)		
AC	11 (20.4%)	4 (16.0%)	7 (24.1%)	7 (41.2%)	<0.0001 [b]	0.09 [b]
SCLC	12 (22.2%)	–	12 (41.4%)	–		
Stage						
I	31 (57.4%)	18 (72.0%)	13 (44.8%)	10 (58.8%)		
II	10 (18.5%)	6 (24.0%)	4 (13.8%)	1 (5.9%)	0.0122 [b]	0.0255 [b]
III	10 (18.5%)	1 (4.0%)	9 (31.0%	5 (29.4%)		
IV	3 (5.6%)	–	3 (10.3%)	1 (5.9%)		
MKI67						
median (Q1;Q3)	6.75 (6.65;6.98)	6.71 (6.65;6.78)	6.87 (6.65;7.43)	6.69 (6.64;6.77)	0.0276 [a]	0.57 [a]
min-max	6.58–8.19	6.58–6.98	6.58–8.19	6.58–7.79		
MCM2						
median (Q1;Q3)	7.33 (7.18;8.39)	7.32 (7.20;7.49)	7.52 (7.10;9.38)	7.15 (7.07;7.25)	0.22 [a]	0.0429 [a]
min-max	6.77–11.11	6.89–7.76	6.77–11.11	6.77–10.93		
PCNA						
median (Q1;Q3)	8.92 (8.52;9.63)	8.69 (8.48;8.98)	9.29 (8.72;10.15)	8.81 (8.46;8.97)	0.0027 [a]	0.52 [a]
min-max	7.81–10.80	7.81–9.63	8.18–10.80	8.18–10.42		
CDKN1A						
median (Q1;Q3)	9.68 (8.94;10.58)	9.46 (8.67;9.78)	10.01 (9.45;10.70)	9.56 (9.05;10.01)	0.0009 [a]	0.18 [a]
min-max	8.43–11.23	8.43–10.61	8.57–11.23	8.57–11.07		
CDKN1B						
median (Q1;Q3)	8.82 (8.46;9.23)	8.50 (8.33;8.74)	9.21 (8.96;9.79)	9.03 (8.46;9.09)	<0.0001 [a]	0.0197 [a]
min-max	6.87–10.18	6.87–9.14	8.07–10.18	8.07–10.01		
Prognosis events						
Death	28 (51.9%)	7 (28.0%)	21 (72.4%)	9 (52.9%)	0.0023 [b]	0.12 [b]
Recurrence	9 (16.7%)	2 (8.0%)	7 (24.1%)	2 (11.8%)	0.15 [b]	1.00 [b]

Percentages could not add up to 100 due to rounding; [a] Wilcoxon test; [b] Fisher's exact test; CL1: cluster 1; CL2: cluster 2; TC: typical carcinoid; AC: atypical carcinoid; SCLC: small cell lung carcinoma; MKI67: marker of proliferation Ki-67; MCM2: minichromosome maintenance complex component 2; PCNA: proliferating cell nuclear antigen; CDKN1A/1B: cyclin dependent kinase inhibitor 1A/1B.

3.3. Clinicopathologic associations and survival analysis

No significant association of clustering and age at surgery, gender, smoking status and pack-year was observed (Table 1). Remarkably, a higher prevalence of stage I-II tumors were detected in CL1, with a relative higher proportion of stage III-IV tumors in CL2, even after excluding SCLC ($p = 0.0255$) (Table 1). Levels of *MKI67*, *PCNA* and *CDKN1A/p21* expression were isoregulated between CL1 and CL2 carcinoids, while *MCM2* and *CDKN1B/p27* were down- and upregulated in the latter, respectively (Table 1).

Histology-related univariate survival analysis showed a better prognosis for carcinoids as a whole without significant differences between TC and AC (Fig. 2E, Table 2). Interestingly, survival analysis according to clustering showed for CL1 the best prognosis, whereas CL2 as a whole showed a 4.42-fold increased risk of death (Fig. 2F, Table 2), with carcinoid CL2 and SCLC exhibiting an intermediate and the lowest probability of survival, respectively (Fig. 2F).

A significantly impaired survival was observed for older patients at surgery and current smokers, whilst a borderline increased risk of death was detected for stage IV tumors (Table 2). After adjustment for these clinico-pathological risk factors, the hazard ratio for clustering was stable and independently associated to survival, with CL2 showing a 4.48-fold increased risk. After combining the histological type and cluster, the role of CL2 in identifying the subgroup at worse survival was confirmed, with either TC or AC in CL2 (but not AC in CL1) and SCLC (all belonging to CL2) being at increased risk of death in an independent way (Table 2). Similar results were partly obtained in the independent cohort of 101 NENs (Fig. S3 E; Supplemental Table 3A), despite prognostic significance of CL2 was not reached in multivariate analysis probably due to the limited number of carcinoids ($N = 24$, 12 in CL1 and only 2 in CL2) (Supplemental Table 3B-C).

Prognostic analysis of GSE118131 cohort was not performed due to the lack of available survival data, but the cluster subdivision was strikingly similar. It is worth mentioning that in the context of lung carcinoids, where prognosis is generally more favorable as compared to NECs, the evaluation of disease-related mortality and recurrence-free survival could represent complementary end points. Unfortunately, we could not evaluate such aspects due to the lack of information on causes of death and just partial details on recurrence time. However, when we investigated the distribution of cancer recurrences according to cluster analysis, we confirmed a trend towards worse prognosis for CL2 carcinoids, with an intermediate behavior between CL1 and SCLC (Table 1).

4. Discussion

Herein we provide further evidence supporting the existence of a

A

27-gene Lung-NETs signature

Gene	Mut # (CL2/CL1)	Mut Freq. Fold (CL2/CL1)
TSC2	7/1	3.50
SMARCA2	6/1	3.00
ERBB4	7/1	2.00
PTPRZ1	7/2	1.75
SMARCA4	6/2	1.50
LRP1B	8/3	1.33
ARID2	5/2	1.25
RB1	5/2	1.25
ARID1B	7/3	1.17
KMT2D	7/3	1.17
NOTCH2	7/3	1.17
SPHKAP	7/3	1.17
THSD7B	7/3	1.17
ARID1A	8/4	1.00
CSMD3	8/4	1.00
KMT2C	8/4	1.00
PCLO	8/4	1.00
PIK3CA	6/3	1.00
SETD2	8/4	1.00
DSCAML1	7/4	0.88
ATM	6/4	0.75
PBRM1	5/4	0.63
TP53	2/2	0.50
MEN1	3/2	0.33
NCAM2	1/1	0.13
KRAS	1/0	0.00
STK11	0/0	N.D.

B

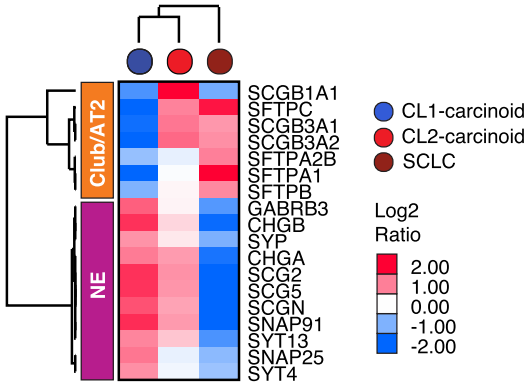

C

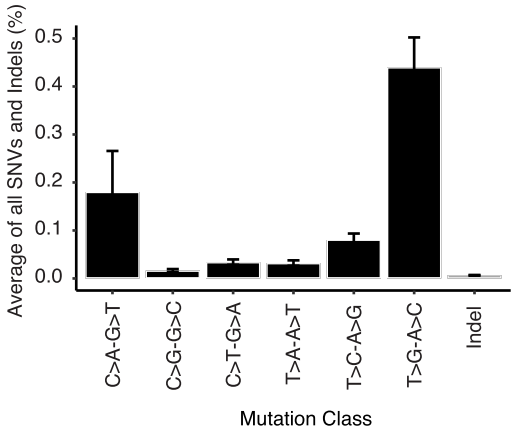

D

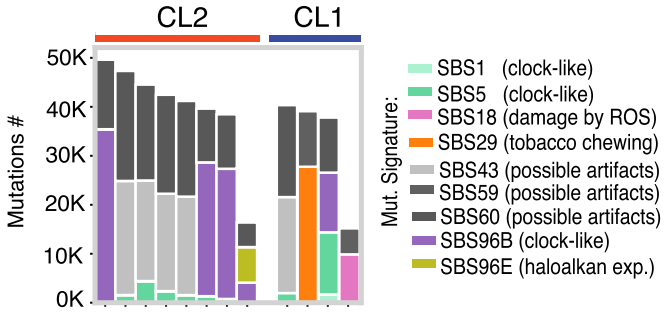

E

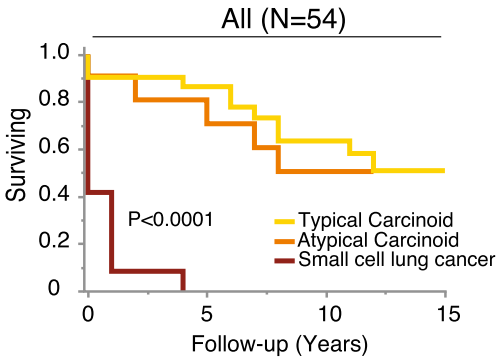

F

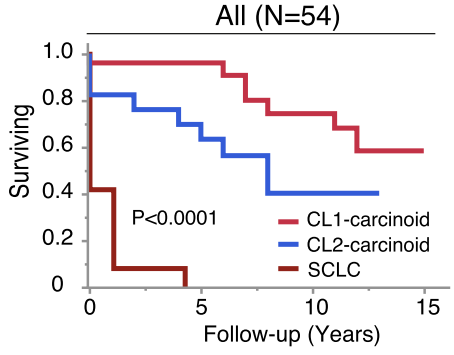

(caption on next page)

Fig. 2. A. Frequency of mutations (mut) of the 27-gene signature previously found altered in NETs. The number of mutations as well as the fold difference (ratio) of mut frequency in CL2-carcinoids vs. CL1-carcinoids are shown. B. Hierarchical clustering analysis of the expression profile of genes related to different lung cell lineages. NE, neuroendocrine cells. Club/AT2, club cells or alveolar type 2 cells, respectively. Color code is as per the legend. C. Pattern of mutational substitutions identified in the Asiedu's (Asiedu et al., 2018) samples by whole-exome sequencing analysis. Bar plot indicate the average of percentage of SNVs and Indels over the samples analyzed ($N = 12$). Error bars indicate relative standard errors. D. Single base substitution (SBS) distribution in the Asiedu's (Asiedu et al., 2018) samples (N = 12) divided into CL1 and CL2. Color codes are as per the legend. E. Kaplan-Meier plot indicating the overall survival of patients ($N = 54$) with different NET subtypes. Color codes are as per the legend. Statistical significance was calculated by log-rank test. F. Kaplan-Meier plot indicating the overall survival of patients (N = 54) with different CL1- or CL2-carcinoids or SCLC. Color codes are as per the legend. Statistical significance was calculated by log-rank test.

subset of NETs closely akin to aggressive neuroendocrine neoplasms in terms of both molecular features and prognostic outcome. We previously identified a gene signature whose alterations hallmarked lung carcinoids showing aggressive clinical behavior, thereby supporting an innovative concept of evolving or secondary high-grade (poorly differentiated) neuroendocrine neoplasms (S-PDNENs), namely secondary NECs (S-NECs). When the expression pattern of such gene signature was generalized to three independent cohorts of lung NENs also comprising 53 carcinoids, we confirmed the existence of a subset of tumors prone to transformation we called CL2, inasmuch as was intertwined with SCLC and LCNEC in the same cluster and showed high proliferation and HPCS biomarkers. Consistently with our previous findings (Pelosi et al., 2018), multivariable survival analysis confirmed CL2 carcinoids as an independent life-threatening tumor group, with an intermediate prognosis between steady-state carcinoids of the cluster CL1 and NECs belonging to the same cluster.

Yet, CL2-carcinoids had a distinct transcriptional profile as compared to CL1-carcinoids, with hundreds of genes differing between them despite similar histologic features, which in turn impacted on molecular mechanisms involved in cell proliferation, metabolism and inflammation. Interestingly, we noted that this aggressive subset of NETs had TIL-specific gene signatures characteristic of CD8+ T-cell exhaustion, which is considered a hallmark of cancer progression (Thommen and Schumacher, 2018). As a matter of fact, we identified a higher mutation rate of *TSC2* gene in CL2-carcinoids, where Tuberous sclerosis complex subunit 1 (*TSC1*) and 2 (*TSC2*) gene loss of function has been associated with an inflamed microenvironment due to increase of cell surface protein expression of the programmed cell death ligand 1 (PD-L1), a promoter of immune system exhaustion responsible for clinical benefit and increased survival in NSCC patients treated with anti-PD-1/PD-L1 therapy (Huang et al., 2022).

Mutational profile of CL2-carcinoids also revealed a higher rate of mutations in genes involved in epigenetic mechanisms responsible for driving lung tumor cell plasticity, such as *SMARCA2* and *SMARCA4*, in both NENs (Rekhtman, 2022) and NSCC (Dagogo-Jack et al., 2020; Rekhtman et al., 2020). Indeed, CL2-carcinoids were found to be enriched in signatures associated with stemness, EMT and HPCS (Marjanovic et al., 2020) (Fig. S1 E,F), as well as in downregulation of neuroendocrine markers (chromogranins and synaptophysin) and upregulation of adenocarcinoma markers of AT2 club cells. Modulation of stem cell activity and HPCS with protumorigenic properties of molecularly heterogeneous cell populations (Zhang et al., 2018) was also hypothesized by upregulation of cell proliferation-related markers *MKI67* and *PCNA* in CL2 carcinoids (Table 1) but downregulation of *MCM2* (an initiator of eukaryotic genome replication) (Yu et al., 2020), which could promote stemness and aging/clock-like phenotype (Pruitt et al., 2007; Xu et al., 2022) (Fig. 2D). Likewise, we found that *CDKN1A-1B/p21*-p27 upregulation, two inhibitors of cell cycle progression involved in progenitor/stem cell fate and specification (Andreu et al., 2015) (Table 1), were also in keeping with our previous observations of low proliferative activity of carcinoid-looking NETs molecularly straddling LCNECs [the so-called pulmonary supra-carcinoids (Alcala et al., 2019)].

Our working hypothesis on NET transdifferentiation towards S-PDNENs, i.e., S-NECs, (Dinter et al., 2019; Fabbri et al., 2017; Pelosi et al., 2021; Pelosi et al., 2018; Volante et al., 2021), which however still needs formal demonstration on experimental models, would include downregulation of neuroendocrine markers along with upregulation of AT2 club cell traits in CL2-carcinoids (Fig. 2 B, Supplementary Table 1), thereby speculating on the role of master regulators *YAP/TAZ* in the stepwise evolution of NETs to less neuroendocrine-differentiated SCLC molecularly akin to non-small cell carcinoma with adenocarcinoma lineage through *MYC* and *NOTCH* activation, as reported by others (Ireland et al., 2020; Owonikoko et al., 2021; Wu et al., 2021). As a matter of fact, we observed that CL2 NENs (grouping carcinoids and SCLC) also featured predicted activation of *YAP1* (Supplementary Table 2) along with *MYC* and *NOTCH1* upregulation and *NOTCH2* mutation (|1.17| fold change, Fig. 1 A-B and Fig. 2 A (Hong et al., 2022), thus suggesting different steps of evolution from NETs via MYC/NOTCH signaling towards less NE-differentiated tumors. Other findings in CL2 NENs, such as EZH2 upregulation (a suppressor of adaptive antitumor *immune response,* data not shown) (Mahadevan et al., 2021), downregulation of tumor-killing M1 macrophages (Zheng et al., 2021) (Fig. 1E), accumulation of M1 macrophages as a natural filter to avoid cancer stem cells being eliminated (Liu et al., 2021), enrichment in CD8+ T-cells and M2 macrophages (Fig. 1E), and *YAP1* (Baine et al., 2020; Gay et al., 2021; Owonikoko et al., 2021) expression (Supplementary Table 2), are all in keeping with immune system anergy being epigenetically involved in this transition towards these less NE differentiated tumors somewhat akin to non-small cell carcinoma, which in turn results in survival impairment enhanced chemoresistance but, likely, more effectiveness of immunotherapy (Gay et al., 2021; Rudin et al., 2023).

In such scenario, we would like to observe that CL2 carcinoids sharing molecular features of high-grade neuroendocrine neoplasms were likely to show characters of tumor cell plasticity, proliferation and immune system exhaustion. Of note, mutations were predominantly T > C or C > T transitions deriving from DNA mismatch repair pathway activation, haloalkane signature and age-related events, thus suggesting endogenous or exogenous mutational events in the population of steady-state carcinoids able to promote expansion through epigenetic mechanisms of the genetically more heterogeneous CL2 carcinoids at risk of further evolution to NECs through acquisition of NEC-like properties (Cros et al., 2021). In this regard, S-PDNENs, i.e., S-NECs, would make up a family of lesions unified by diverse evolutionary trajectories stemming from different ancestors such as carcinoids or NSCC towards SCLC- or LCNEC-looking neoplasms, in pure or combined forms, depending on the different timing of activated gene signatures (Meder et al., 2016; Metovic et al., 2021b; Pelosi, 2022; Pelosi et al., 2021; Pelosi et al., 2018; Pelosi et al., 2019). In this regard, HPCS and immune system anergy could favor tumorigenesis, as recently suggested for pollution and lung adenocarcinoma development (Hill et al., 2023).

The simplicity of our gene signature to distinguish CL2 carcinoids sharing molecular features of high-grade neuroendocrine neoplasms makes our findings worthwhile reporting, despite severe limitations due to its retrospective character, small number of analyzed tumors and the lack of disease-free survival data and of direct demonstration of carcinoid transition to NECs by means of experimental models rather than an in silico analysis of already published data (Pelosi et al., 2021; Pelosi et al., 2018).

Author contribution statement

Giuseppe Pelosi and Fabrizio Bianchi: conceptualization,

Table 2
Univariate and multivariable Cox regression analysis.

			Univariate analysis		Multivariable analysis (histologic type and cluster not combined)		Multivariable analysis (histologic type and cluster combined)	
	N = 54	N. of deaths = 28	HR (95% CI)	Wald test	HR (95% CI)	Wald test	HR (95% CI)	Wald test
Age at surgery (for 1 unit increase)	54	28	**1.08 (1.03–1.12)**	**0.0003**	**1.07 (1.02–1.13)**	**0.0034**	**1.08 (1.03–1.14)**	**0.0031**
Male (vs female)	20	9	0.77 (0.35–1.70)	0.51	0.71 (0.28–1.80)	0.47	0.70 (0.27–1.79)	0.46
Former smoker (vs never smoker)	20	13	2.16 (0.86–5.42)	0.10	2.48 (0.82–7.53)	0.11	2.86 (0.88–9.34)	0.08
Current smoker (vs never smoker)	11	8	**3.57 (1.28–9.95)**	**0.0148**	1.84 (0.42–8.00)	0.42	2.10 (0.46–9.62)	0.34
Stage II (vs stage I)	10	5	1.21 (0.43–3.36)	0.72	1.85 (0.50–6.76)	0.35	2.28 (0.54–9.56)	0.26
Stage III (vs stage I)	10	6	1.71 (0.65–4.46)	0.28	0.93 (0.26–3.35)	0.91	1.03 (0.27–3.85)	0.97
Stage IV (vs stage I)	3	3	3.34 (0.95–11.76)	0.06	0.78 (0.15–3.99)	0.77	0.78 (0.15–4.01)	0.77
AC (vs TC)	11	5	1.33 (0.46–3.87)	0.60	0.99 (0.32–3.06)	0.99	–	
SCLC (vs TC)	12	12	**13.71 (4.49–41.90)**	**<0.0001**	3.96 (0.68–23.05)	0.13		
Cluster CL2 (vs CL1)	29	21	**4.42 (1.84–10.63)**	**0.0009**	**4.48 (1.34–14.97)**	**0.0148**	–	
TC CL2 (vs TC CL1)	10	5	2.86 (0.85–9.56)	0.0886	–		**3.81 (1.03–14.04)**	**0.0449**
AC CL1 (vs TC CL1)	4	1	1.03 (0.12–8.62)	0.98			0.50 (0.05–5.22)	0.56
AC CL2 (vs TC CL1)	7	4	2.45 (0.68–8.78)	0.17			**5.16 (1.18–22.66)**	**0.0297**
SCLC CL2 (vs TC CL1)	12	12	**20.86 (5.81–74.92)**	**<0.0001**			**14.64 (2.46–87.26)**	**0.0032**

TC: typical carcinoid; AC: atypical carcinoid; SCLC: small cell lung carcinoma; CL1: cluster 1; CL2: cluster 2.

methodology, original draft preparation, review, editing and manuscript finalization; Elisa Dama, Valentina Melocchi, and Fabrizio Bianchi: bioinformatics and statistical analyses performance; Paul Hofman, Marco De Luca, Adriana Albini, Maria Gemelli, Riccardo Ricotta, Mauro Papotti, Angelica Sonzogni, Stefano La Rosa, Silvia Uccella, Sergio Harari: critical review, editing and manuscript finalization; Michael K. Asiedu, Dennis A. Wigle: molecular, clinical and pathology data collection, critical review and manuscript finalization.

Funding

This work was supported by the Italian Ministry of Health (Ricerca Corrente; RF-2021-12372433 to FB), by the Italian Ministry of Education, University and Research (MIUR) [PON BIO-D to F.B.], and by the Associazione Italiana Ricerca sul Cancro [IG-22827 to F.B.]. The study funders had no role in the design of the study, collection, analysis, and interpretation of the data, writing of the manuscript, and decision to submit the manuscript for publication.

Ethical approval

This study delt with reanalysis of previously generated and authorized molecular and clinical information by the Internal Review Boards of the participating Institutions (Asiedu et al., 2018; Pelosi et al., 2018), thus no further ethics release was necessary.

CRediT authorship contribution statement

Giuseppe Pelosi: Conceptualization, Data curation, Formal analysis, Investigation, Methodology, Supervision, Validation, Visualization, Writing – original draft, Writing – review & editing. **Valentina Melocchi:** Supervision, Validation, Visualization, Writing – review & editing. **Elisa Dama:** Supervision, Validation, Visualization, Writing – review & editing. **Paul Hofman:** Supervision, Validation, Visualization, Writing – review & editing. **Marco De Luca:** Conceptualization, Supervision, Validation, Visualization, Writing – review & editing. **Adriana Albini:** Supervision, Validation, Visualization, Writing – review & editing. **Maria Gemelli:** Supervision, Validation, Visualization, Writing – review & editing. **Riccardo Ricotta:** Supervision, Validation, Visualization, Writing – review & editing. **Mauro Papotti:** Software, Supervision, Validation, Visualization, Writing – review & editing. **Stefano La Rosa:** Supervision, Validation, Visualization, Writing – review & editing. **Silvia Uccella:** Supervision, Validation, Visualization, Writing – review & editing. **Sergio Harari:** Supervision, Validation, Visualization, Writing – review & editing. **Angelica Sonzogni:** Supervision, Validation, Visualization, Writing – review & editing. **Michael K. Asiedu:** Data curation, Formal analysis, Supervision, Validation, Visualization, Writing – review & editing. **Dennis A. Wigle:** Data curation, Formal analysis, Supervision, Validation, Visualization, Writing – review & editing. **Fabrizio Bianchi:** Conceptualization, Data curation, Formal analysis, Funding acquisition, Investigation, Methodology, Software, Supervision, Validation, Visualization, Writing – original draft, Writing – review & editing.

Declaration of competing interest

The author has no relevant affiliations or financial involvement with any organization or entity with a financial interest in or financial conflict with the subject matter or materials discussed in the manuscript. This includes employment, consultancies, honoraria, stock ownership or options, expert testimony, grants or patents received or pending, or royalties.

Data availability

Datasets are available from GEO database (https://www.ncbi.nlm.nih.gov/gds) with the following accession numbers: GSE108055, GSE30219, GSE118131.

Acknowledgments

This work is dedicated to the memory of Carlotta, an extraordinarily lively girl who died an untimely death due to cancer in the prime of her life.

Appendix A. Supplementary data

Supplementary data to this article can be found online at https://doi.org/10.1016/j.yexmp.2024.104882.

References

Alcala, N., et al., 2019. Integrative and comparative genomic analyses identify clinically relevant pulmonary carcinoid groups and unveil the supra-carcinoids. Nat. Commun. 10, 3407.
Alexandrov, L.B., et al., 2016. Mutational signatures associated with tobacco smoking in human cancer. Science. 354, 618–622.
Alexandrov, L.B., et al., 2020. The repertoire of mutational signatures in human cancer. Nature. 578, 94–101.
Alvisi, G., et al., 2020. IRF4 instructs effector Treg differentiation and immune suppression in human cancer. J. Clin. Invest. 130, 3137–3150.

Andreu, Z., et al., 2015. The cyclin-dependent kinase inhibitor p27 kip1 regulates radial stem cell quiescence and neurogenesis in the adult hippocampus. Stem Cells 33, 219–229.
Asiedu, M.K., et al., 2018. Pathways impacted by genomic alterations in pulmonary carcinoid tumors. Clin. Cancer Res. 24, 1691–1704.
Baine, M.K., et al., 2020. SCLC subtypes defined by ASCL1, NEUROD1, POU2F3, and YAP1: a comprehensive immunohistochemical and histopathologic characterization. J. Thorac. Oncol. 15, 1823–1835.
Beasley, M.B., et al., 2021. Small cell lung carcinoma. In: WHO Classification of Tumours Editorial Board. Toracic Tumour, , 5th edvol. 5. International Agency for Research on Cancer, Lyon (France), pp. 139–143. WHO classification of tumor series.
Chang, L., et al., 2018. The SWI/SNF complex is a mechanoregulated inhibitor of YAP and TAZ. Nature. 563, 265–269.
Concepcion, C.P., et al., 2022. Smarca4 inactivation promotes lineage-specific transformation and early metastatic features in the lung. Cancer Discov. 12, 562–585.
Cros, J., et al., 2021. Specific genomic alterations in high-grade pulmonary neuroendocrine Tumours with carcinoid morphology. Neuroendocrinology. 111, 158–169.
Dagogo-Jack, I., et al., 2020. Clinicopathologic characteristics of BRG1-deficient NSCLC. J. Thorac. Oncol. 15, 766–776.
Dinter, H., et al., 2019. Molecular classification of neuroendocrine tumors of the Thymus. J. Thorac. Oncol. 14, 1472–1483.
Fabbri, A., et al., 2017. Thymus neuroendocrine tumors with CTNNB1 gene mutations, disarrayed ss-catenin expression, and dual intra-tumor Ki-67 labeling index compartmentalization challenge the concept of secondary high-grade neuroendocrine tumor: a paradigm shift. Virchows Arch. 471, 31–47.
Gay, C.M., et al., 2021. Patterns of transcription factor programs and immune pathway activation define four major subtypes of SCLC with distinct therapeutic vulnerabilities. Cancer Cell 39 (346–360), e7.
Hill, W., et al., 2023. Lung adenocarcinoma promotion by air pollutants. Nature. 616, 159–167.
Hong, D., et al., 2022. Plasticity in the absence of NOTCH uncovers a RUNX2-dependent pathway in small cell lung Cancer. Cancer Res. 82, 248–263.
Huang, Q., et al., 2022. Loss of TSC1/TSC2 sensitizes immune checkpoint blockade in non-small cell lung cancer. Sci. Adv. 8 (5), eabi9533.
Ireland, A.S., et al., 2020. MYC drives temporal evolution of small cell lung Cancer subtypes by reprogramming neuroendocrine fate. Cancer Cell 38 (60–78), e12.
Kadoch, C., et al., 2013. Proteomic and bioinformatic analysis of mammalian SWI/SNF complexes identifies extensive roles in human malignancy. Nat. Genet. 45, 592–601.
Laddha, S.V., et al., 2019. Integrative genomic characterization identifies molecular subtypes of lung carcinoids. Cancer Res. 79, 4339–4347.
Li, H., Durbin, R., 2009. Fast and accurate short read alignment with burrows-wheeler transform. Bioinformatics. 25, 1754–1760.
Liu, J., et al., 2021. New insights into M1/M2 macrophages: key modulators in cancer progression. Cancer Cell Int. 21 (1), 389.
Luchtenborg, M., et al., 2014. Survival of patients with small cell lung cancer undergoing lung resection in England, 1998-2009. Thorax. 69, 269–273.
Mahadevan, N.R., et al., 2021. Intrinsic immunogenicity of small cell lung carcinoma revealed by its cellular plasticity. Cancer Discov. 11, 1952–1969.
Marjanovic, N.D., et al., 2020. Emergence of a high-plasticity cell state during lung cancer evolution. Cancer Cell 38 (229–246), e13.
Meder, L., et al., 2016. NOTCH, ASCL1, p53 and RB alterations define an alternative pathway driving neuroendocrine and small cell lung carcinomas. Int. J. Cancer 138, 927–938.
Metovic, J., et al., 2021a. Morphologic and molecular classification of lung neuroendocrine neoplasms. Virchows Arch. 478, 5–19.
Metovic, J., et al., 2021b. Recent advances and current controversies in lung neuroendocrine neoplasms. Semin. Diagn. Pathol. 38, 90–97.
Newman, A.M., et al., 2019. Determining cell type abundance and expression from bulk tissues with digital cytometry. Nat. Biotechnol. 37, 773–782.
Owonikoko, T.K., et al., 2021. YAP1 expression in SCLC defines a distinct subtype with T-cell-inflamed phenotype. J. Thorac. Oncol. 16, 464–476.
Papotti, M., et al., 2021. Carcinoid/neuroendocrine tumour of the lung. In: WHO Classification of Tumours Editorial Board. Toracic Tumour, , 5th edvol. 5. International Agency for Research on Cancer, Lyon (France), pp. 133–138. WHO classification of tumor series.
Parker, R.C., et al., 1981. Cellular homologue (c-src) of the transforming gene of Rous sarcoma virus: isolation, mapping, and transcriptional analysis of c-src and flanking regions. Proc. Natl. Acad. Sci. U. S. A. 78, 5842–5846.
Pelosi, G., 2022. The natural history in lung neuroendocrine neoplasms: the stone guest who matters. J. Thorac. Oncol. 17, e5–e8.
Pelosi, G., et al., 2017. Classification of pulmonary neuroendocrine tumors: new insights. Transl. Lung Cancer Res. 6, 513–529.
Pelosi, G., et al., 2018. Most high-grade neuroendocrine tumours of the lung are likely to secondarily develop from pre-existing carcinoids: innovative findings skipping the current pathogenesis paradigm. Virchows Arch. 472, 567–577.
Pelosi, G., et al., 2019. Recent advances in the molecular landscape of lung neuroendocrine tumors. Expert. Rev. Mol. Diagn. 19, 281–297.
Pelosi, G., et al., 2021. A subset of large cell neuroendocrine carcinomas in the Gastroenteropancreatic tract may evolve from pre-existing well-differentiated neuroendocrine tumors. Endocr. Pathol. 32, 396–407.
Peng, W., et al., 2022. Comprehensive characterization of the genomic landscape in Chinese pulmonary neuroendocrine tumors reveals prognostic and therapeutic markers (CSWOG-1901). Oncologist 27 (2), e116–e125.
Petrella, F., et al., 2022. The role of surgery in high-grade neuroendocrine cancer: indications for clinical practice. Front Med (Lausanne). 9, 869320.
Pleasance, E.D., et al., 2010. A small-cell lung cancer genome with complex signatures of tobacco exposure. Nature. 463, 184–190.
Pruitt, S.C., et al., 2007. Reduced Mcm2 expression results in severe stem/progenitor cell deficiency and cancer. Stem Cells 25, 3121–3132.
Rekhtman, N., 2022. Lung neuroendocrine neoplasms: recent progress and persistent challenges. Mod. Pathol. 35, 36–50.
Rekhtman, N., et al., 2020. SMARCA4-deficient thoracic Sarcomatoid tumors represent primarily smoking-related undifferentiated carcinomas rather than primary thoracic sarcomas. J. Thorac. Oncol. 15, 231–247.
Rekhtman, N., et al., 2021. Large cell neuroendocrine carcinoma of the lung. In: WHO Classification of Tumours Editorial Board. Toracic Tumour, , 5th edvol. 5. International Agency for Research on Cancer, Lyon (France), pp. 144–149. WHO classification of tumor series.
Rousseaux, S., et al., 2013. Ectopic activation of germline and placental genes identifies aggressive metastasis-prone lung cancers. Sci. Transl. Med. 5 (186), 186ra66.
Rubin, M.A., et al., 2020. Impact of lineage plasticity to and from a neuroendocrine phenotype on progression and response in prostate and lung cancers. Mol. Cell 80, 562–577.
Rudin, C.M., et al., 2023. Clinical benefit from immunotherapy in patients with SCLC is associated with tumor capacity for antigen presentation. J. Thorac. Oncol. 18, 1222–1232.
Shao, X., et al., 2019. Copy number variation is highly correlated with differential gene expression: a pan-cancer study. BMC Med. Genet. 20 (1), 175.
Simbolo, M., et al., 2019. Gene expression profiling of lung atypical carcinoids and large cell neuroendocrine carcinomas identifies three transcriptomic subtypes with specific genomic alterations. J. Thorac. Oncol. 14, 1651–1661.
Thommen, D.S., Schumacher, T.N., 2018. T cell dysfunction in cancer. Cancer Cell 33, 547–562.
Travis, W., et al., 2021. Lung neuroendocrine neoplasms: Introduction. In: WHO Classification of Tumours Editorial Board. Toracic Tumour, , 5th edvol. 5. International Agency for Research on Cancer, Lyon (France), pp. 127–129. WHO classification of tumor series.
Van der Auwera, G.A., et al., 2013. From FastQ data to high confidence variant calls: the genome analysis toolkit best practices pipeline. Curr. Protoc. Bioinformatics 43 (1110), 11.10.1–11.10.33.
Volante, M., et al., 2021. Molecular pathology of well-differentiated pulmonary and Thymic neuroendocrine tumors: what do pathologists need to know? Endocr. Pathol. 32, 154–168.
Vollbrecht, C., et al., 2015. Mutational analysis of pulmonary tumours with neuroendocrine features using targeted massive parallel sequencing: a comparison of a neglected tumour group. Br. J. Cancer 113, 1704–1711.
Wu, Q., et al., 2021. YAP drives fate conversion and chemoresistance of small cell lung cancer. Sci. Adv. 7 (40), eabg1850.
Xu, X., et al., 2022. Mcm2 promotes stem cell differentiation via its ability to bind H3-H4. Elife. 11, e80917.
Yu, S., et al., 2020. MCMs in Cancer: prognostic potential and mechanisms. Anal. Cell. Pathol. (Amst.) 2020, 3750294.
Zhang, W., et al., 2018. Small cell lung cancer tumors and preclinical models display heterogeneity of neuroendocrine phenotypes. Transl. Lung Cancer Res. 7, 32–49.
Zheng, Y., et al., 2021. Epigenetic silencing of chemokine CCL2 represses macrophage infiltration to potentiate tumor development in small cell lung cancer. Cancer Lett. 499, 148–163.